Journal of Reproduction and Development, Vol. 67, No 6, 2021

Original Article

Effects of electromagnetic waves on oocyte maturation and embryonic development in pigs

Jia-Si CHEN[1)], Li-Kuang TSAI[2)], Ting-Yu YEH[3)], Tzai-Shiuan LI[1)], Cheng-Han LI[4)], Zung-Hang WEI[5)], Neng-Wen LO[6)] and Jyh-Cherng JU[1, 7–9)]

[1)]*Graduate Institute of Biomedical Sciences, China Medical University, Taichung 40402, Taiwan*
[2)]*Institute of Biotechnology, National Taiwan University, Taipei 10617, Taiwan*
[3)]*Ph.D. Program in Tissue Engineering and Regenerative Medicine, National Chung Hsing University, Taichung 40227, Taiwan*
[4)]*Department of Bio-Industrial Mechatronics Engineering, National Chung Hsing University, Taichung 40227, Taiwan*
[5)]*Department of Research and Development, Weistron Co., Ltd., Hsinchu 30013, Taiwan*
[6)]*Department of Animal Science and Biotechnology, Tunghai University, Taichung 40704, Taiwan*
[7)]*Translational Medicine Research Center, China Medical University Hospital, Taichung 40402, Taiwan*
[8)]*Department of Animal Science, National Chung Hsing University, Taichung 40227, Taiwan*
[9)]*Department of Bioinformatics and Medical Engineering, Asia University, Taichung 41354, Taiwan*

Abstract. Our living environment has been full of electromagnetic radiation (EMR) due to the prevailing electronic devices and equipment. Intermediate frequency electromagnetic field (IF-EMF) or waves constitute a significant part of EMR; therefore, an increasing number of household electrical appliances have become a source of IF-EMF, and concerns about IF-EMF on health are gaining more attention. However, little information is available about its impact on female reproductive traits, such as germ cell viability and early embryonic development, particularly at the cellular and molecular levels. In this study, we used porcine oocytes as a model system to explore the effect of IF-EMF at various intensities on the *in vitro* maturation (IVM) of oocytes and their subsequent embryonic development. Our results showed that no difference in oocyte maturation rates was detected among groups, but the cleavage and blastocyst rates of parthenotes derived from EMF-treated oocytes decreased with the weaker IF-EMF intensity (25 and 50 Gauss) groups compared to the control group ($P < 0.05$). For cytoplasmic maturation, the weaker IF-EMF intensity groups also showed a peripheral pattern of mitochondrial distribution resembling that of immature oocytes and increased autophagy activity. No obvious differences in cytoskeletal distribution and total cell numbers of blastocysts were investigated in the four IF-EMF treatments compared to those in the control group. Although the underlying mechanism associated with EMF effects on oocytes and embryos is still elusive, we have demonstrated that low intensity IF-EMF exerts harmful effects on porcine oocytes during the maturation stage, carrying over such effects to their subsequent embryonic development.

Key words: Alternating magnetic field, Autophagy, *In vitro* maturation, Mitochondria, Porcine oocytes

(**J. Reprod. Dev. 67:** 392–401, 2021)

The effects of extremely low-frequency electromagnetic fields (ELF-EMFs) on animals or humans at the cellular level or even in the whole organism have been investigated for decades [1–5]. Similarly, the attention to intermediate frequency EMF (IF-EMF) has been increasing recently, while the use of electrical appliances has been widespread in households. IF-EMF is defined as a frequency ranging from 300 Hz to 10 MHz. The safe limit of exposure to this type of radiation in the guidelines of the International Commission on Non-Ionizing Radiation Protection (ICNIRP) is 27 μT (ICNIRP, 2010 and 2013). It is known that induction heaters, electronic article surveillance (EAS) systems, wireless power transfer, and other such technologies are the universal sources of IF-EMF in our daily life [6, 7].

Received: June 13, 2021
Accepted: September 23, 2021
Advanced Epub: October 23, 2021

Correspondence: JC Ju (e-mail: jcju@mail.cmu.edu.tw; jcju@dragon.nchu.edu.tw)

Most previous studies have verified no severe harmful effects or toxicity at the cellular level, such as cell proliferation, differentiation, apoptosis, genetic injury, DNA damage, and even cell cycle distribution in various species such as mice, rats, and humans under IF-EMF exposure [8–12]. It is noteworthy that rat cells exposed to 7.5 kHz IF-EMF at various intensities for 24 h or 5 weeks had an increased cell proliferation or suppressed cell death [9]. In addition, an *in vivo* study showed that the absence of acute or subchronic cytotoxicity was detectable under IF-EMF exposure for 14 days or 3 weeks upon histopathological analysis [13]. Similar results were also reported by Kim *et al*. (2006) [14].

As for the male reproductive system, when mice were exposed at 7.5 kHz under 12, or 120 μT IF-EMF for five weeks, no adverse effects on sperm fertility-related parameters, including total sperm counts and sperm abnormality were found; instead, increased sperm motility was observed [15]. No discernible adverse effects on fetal development or organogenesis were observed for pregnant animals subjected to IF-EMF for a short period or even a whole gestation period [16–20]. One study also revealed that no observable harm to embryonic day (E) 18 fetuses indirectly exposed to 20 kHz IF-EMF at 30 μT could be detected, but the authors indicated that a strain-

specific sensitivity existed because of different results reported in previous studies [21]. Moreover, there were no differences in the risk of miscarriage, birth weight reduction, and preterm birth between female cashiers in different store types whether EAS devices were used or not [22].

The quality of *in vitro*-produced porcine oocytes is significantly lower than those of their *in vivo* counterparts, where better cytoplasmic maturation may be one of the main contributors to this phenomenon [23]. For *in vitro* matured oocytes, even though they have released the first polar bodies and reach nuclear maturation, cytoplasmic maturation is often incomplete. Cytoplasmic maturation is influenced by specific signaling molecules and the dynamic migration of organelles; hence, the mitochondrial patterns, cytoskeleton distribution, apoptosis, ROS production, and autophagy are frequently evaluated to confirm the cytoplasmic maturation of IVM oocytes.

To the best of our knowledge, no report is available on the direct impact of IF-EMF on female germ cell development, particularly in porcine species. In the present study, we aimed to evaluate the effects of various IF-EMF intensities on porcine oocyte maturation and subsequent embryonic development. Maturation rates and alterations in intracellular parameters, including mitochondrial and cytoskeletal distribution, and the expression of autophagy markers, were investigated in porcine oocytes treated with 0, 25, 50, 75 or 100 gauss (G) EMF intensities at 40 kHz IF-EMFs during IVM and after parthenogenetic activation.

Materials and Methods

Chemicals

Unless otherwise indicated, all chemicals used in this study were purchased from Gibco (Thermo Fisher Scientific Inc., Waltham, MA, USA) or Sigma-Aldrich (Merck Group, Damstadt, Germany).

Collection of ovaries and in vitro maturation of oocytes

Fresh ovaries acquired from pre-pubertal gilts in the local slaughterhouse were delivered to the laboratory within 2 h in 39°C normal saline (0.9% w/v NaCl; 0241, VWR Life Science, Avantor Inc., Radnor, PA, USA) supplemented with 0.2% penimycin-S injection (E002123, China Chemical & Pharmaceutical Co., Taipei, Taiwan). Ovaries were rinsed three times with pre-warmed saline. Oocytes were aspirated from ovarian follicles (2–8 mm in diameter) using an 18-G needle attached to a 10 ml syringe. Cumulus oocyte complexes (COCs) with at least three layers of cumulus cells surrounding the homogeneous ooplasm were selected for IVM under a stereomicroscope (SZ61, Olympus Corporation, Tokyo, Japan). Selected COCs were first washed with T10 medium (HEPES-buffered medium 199 (12340-030, Gibco) supplemented with 10% fetal bovine serum (FBS; 10437-028, Gibco) and 1% penicillin/streptomycin (P/S; 15140-122, Gibco) and then with IVM medium (Medium 199 (11150-059, Gibco) supplemented with 10% FBS, 10% porcine follicular fluid, 1% P/S, 10 IU/ml hCG (4778, BioVision, Milpitas, CA, USA) and 10 IU/ml FSH (F2293, Sigma-Aldrich) three times before culture. IVM medium covered with mineral oil (26137-85, Nacalai Tesque, Kyoto, Japan) was equilibrated overnight in an incubator with 5% CO_2 at 39°C. Twenty to thirty COCs were cultured in a 100 µl droplet of IVM medium for 42–44 h. After IVM culture, oocytes were transferred to T10 medium containing 0.1% (w/v) hyaluronidase (H3506, Sigma-Aldrich) and pipetted gently 10-20 times depending on the level of cumulus cell dispersion, and then washed with T10 medium without hyaluronidase. Cumulus cells were completely removed by pipetting up and down with a mouth pipette connected to a narrow glass needle (7095B-5X, Corning Inc., Corning, NY, USA). Mature oocytes with the first polar body were subjected to parthenogenetic activation or fixed in 4% paraformaldehyde (BL0415, Bionovas, Toronto, Canada) for immunocytochemical staining.

Experimental design

Porcine COCs were exposed to IF-EMF during IVM to determine the effects of EMF on oocyte maturation and subsequent embryonic development. COCs from antral follicles were matured *in vitro* during treatment with various EMF intensities, that is, 0, 25, 50, 75, and 100 G. Oocyte maturation rates, mitochondrial localization, cytoskeleton distribution, and the expression of autophagy markers were assessed after IVM. In addition, oocytes with the first polar body were parthenogenetically activated. The subsequent embryonic development, including the cleavage rates (day 2), blastocyst formation rates (day 7), and the total cell count of each blastocyst, were determined.

Mitochondrial staining

After IVM for 44 h, oocytes denuded by removal of cumulus cells were soaked in 4% paraformaldehyde overnight for fixation. The fixed oocytes were washed in PBS (BR110, Biomate, Taipei, Taiwan) containing 1% (w/v) bovine serum albumin (BSA; A7906, Sigma-Aldrich) three times, incubated with 200 nM MitoTracker dye (MitoTracker Green FM; M7514, Invitrogen, Thermo Fisher Scientific Inc.) for 30 min and Hoechst for 15 min, and washed in PBS containing 1% BSA three times after staining. The stained oocytes were placed on slides covered with handmade paraffin wax, filled with PBS, and covered with coverslips gently to maintain the spherical shape of the oocytes. Ten to fifteen series scanning sections through the 3-dimensional structure of matured oocytes were performed via confocal microscopy (SP8 X microscope, Leica Camera AG, Wetzlar, Germany) to examine mitochondrial distribution.

The classification of mitochondrial patterns in the current study was based on the criteria of Gonzalez *et al*. [24], i.e., peripheral, polarized, and diffused types, to classify mitochondrial patterns (Fig. 3A–F). Due to their different levels of maturity, the proportions of oocytes with these patterns differ: immature oocytes frequently show a peripheral pattern while most mature oocytes have either polarized or diffused types of mitochondrial distribution [24–26].

Immunofluorescence staining

After IVM, the oocytes were denuded and fixed in 4% paraformaldehyde overnight. The fixed oocytes were washed thrice in PBS, permeabilized in PBS containing 0.5% Triton X-100 for 1 h, and blocked in PBS containing 1% BSA for 45 min. The blocked oocytes were incubated with primary antibodies against autophagy markers, LC3B (ab48394, Abcam, Cambridge, UK) and mTOR (ab2732, Abcam), respectively, overnight at 4°C. The stained oocytes were washed thrice in PBS containing 1% BSA and incubated with the corresponding secondary antibodies (ab150061 or ab150064, Abcam) for 2 h at 25°C. Finally, the oocytes were washed again in PBS containing 1% BSA three times and then arranged on slides in mounting medium containing DAPI (DAPI Fluoromount-G; 0100-20, SouthernBiotech, Birmingham, AL, USA), covered with coverslips, and pressed appropriately. LC3B and mTOR expression was then observed under an epifluorescence microscope (Nikon Eclipse Ti, Nikon Corporation, Tokyo, Japan). All images were acquired using a Nikon DS-Ri2 camera, and the expression of autophagy markers was quantified as the mean intensity (sum of fluorescence intensity / area of the oocyte) using NIS-Elements BR (version 4.30, Nikon

Corporation).

The procedures, including fixation, permeabilization, blocking, and interaction with antibodies, for cytoskeletal staining were similar to those for autophagy staining, with some differences described as follows. Briefly, denuded oocytes were recovered in IVM medium in a 39°C incubator for at least 2 h for cytoskeletal reorganization. The recovered oocytes were fixed in pre-warmed 4% paraformaldehyde for 40 min in a 39°C water bath. The fixed oocytes were also permeabilized, blocked, and stained with an anti-β-tubulin antibody (10068-1-AP, Proteintech, Rosemont, IL, USA) following the protocol for autophagy staining; however, stained oocytes were incubated with rhodamine-conjugated phalloidin (R415, Invitrogen, Thermo Fisher Scientific Inc.) for 1 h followed by three washes in PBS containing 1% BSA. Eventually, the oocytes were transferred onto slides in a mounting medium containing DAPI covered with coverslips. The localization of cytoskeletal patterns was determined using reconstructed images from ten series sections (each with 1–1.5 μm in thickness) acquired under a confocal microscope.

Oocyte activation and embryo culture

Before performing IVA, mature oocytes with a polar body were recovered from the IVM medium for at least 30 min under the same environment as that used during IVM. Afterwards, oocytes were washed 3–6 times with fresh activation medium composed of 0.3 M D-mannitol (M4125, Sigma-Aldrich), 0.01% (w/v) polyvinyl alcohol (P8136, Sigma-Aldrich), 0.1 mM $MgSO_4$ (M2643, Sigma-Aldrich) and 0.1 mM $CaCl_2$ (C5670, Sigma-Aldrich). Matured oocytes were placed into an electrical chamber (BTX microslides; 45-0104, BTX, Harvard Bioscience, Holliston, MA, USA) containing an activation medium and were aligned manually, activated by a single direct current (DC) pulse (2.2 kV/cm, 30 μsec; ECM 2001 Electro Cell Manipulator, BTX, Harvard Bioscience) and then washed with PZM-3 medium (108 mM NaCl, 10 mM KCl (P5405, Sigma-Aldrich), 0.35 mM KH_2PO_4 (P5655, Sigma-Aldrich), 0.4 mM $MgSO_4$, 25.07 mM $NaHCO_3$ (S5761, Sigma-Aldrich), 1 mM L-glutamine (G8540, Sigma-Aldrich), 5 mM taurine (T8691, Sigma-Aldrich), 0.2 mM sodium pyruvate (P2256, Sigma-Aldrich), 2 mM Ca-(lactate)$_2 \cdot 5H_2O$ (C8356, Sigma-Aldrich), 10 mM MEM non-essential amino acid solution (11140-050, Gibco), 20 mM BME amino acids solution (B6766, Sigma-Aldrich) and 1% P/S) for several times. Before treatment with 6-dimethylaminopurine (6-DMAP; D2629, Sigma-Aldrich), electrical pulse-activated oocytes were rinsed with 2.5 mM 6-DMAP once and then continuously incubated for 4 h with the same 6-DMAP concentration. Next, parthenogenetically activated oocytes were cultured in PZM-3 medium for further development. A solution of the kinase inhibitor 6-DMAP and PZM-3 medium was covered with mineral oil and equilibrated overnight in an incubator before use.

Electromagnetic field device

The device for EMF generation consisted of a high-frequency alternating current (AC) power controller and a copper coil (N=100) covered with an insulation coating. The input voltage of the high-frequency power controller was AC 220 V, and the output frequency of the EMF ranged from 20 to 130 kHz. Such a homemade electric field controller and copper coil could generate 10 to 200 G alternating magnetic field (MF) strength (Fig. 1B–D).

The coil was set in a donut-shaped acrylic water jacket with an outer diameter 220 mm, an inner diameter of 35 mm, and a height of 120 mm to prevent overheating (Fig. 1C and D). The water jacket was filled with circulating water from a constant-temperature water bath (37.5°C) to stabilize the culture temperature at 39°C. The heights of the coil set in the water jacket and one culture dish (with oocytes) were 50 mm and 10 mm, respectively. The oocytes were cultured in culture dishes placed in a coil sitting in the center of the insulating water jacket inside the incubator during IVM (Fig. 1A). Eight dishes can be stacked and cultured to receive various intensities of IF-EMF in this device simultaneously.

For the measurement of voltages and frequencies, a small coil (N = 5) was used to induce an MF generated by the handmade coil, and an oscilloscope (InfiniiVision DS05012A, Agilent Technologies, Santa Clara, CA, USA) was utilized to measure the voltage of the induced EMF. Eventually, the MF intensity was calculated based on Faraday's law of electromagnetic induction (Eq. 1).

$$B = \int \frac{\varepsilon \Delta t}{NA} \quad (1)$$

where B is the MF, ε is the electromotive force, N is the number of turns of the induction coil, and A is the area of the cross-section of the induction coil.

Based on the design of the EMF device, the alternating MF intensity decreases while the MF frequency increases gradually and *vice versa*. In the present study, the frequency of the EMF controller was set to 40 kHz to ensure a constant EMF inside the coil. However, this handmade coil produced various IF-EMF intensities at different positions (heights) of the culture dishes in this coil. Moreover, when the distance from the center of the coil increased (i.e., the position of 2 cm from the bottom of the EMF device) and the IF-EMF intensities decreased proportionally (Table 1). This study was designed to expose the oocytes under 0, 25, 50, 75, or 100 G EMF; therefore, similar intensities at different positions were chosen as IVM treatment groups. In other words, the electromagnetic intensities at positions 0, 2, 5, and 7 cm from the bottom of the EMF device were very close to 75, 100, 50, and 25 G, respectively. A position outside of the device (0 G, i.e., no EMF being detected) was used as a control group. All five treatment groups were performed at the same time in each batch of experiments.

Statistical analysis

Data are presented as the mean ± SEM from at least three biological replicates. Statistically significant differences were assessed using a two-tailed Student's *t*-test using SAS software (version 9.4; SAS Institute, Cary, NC, USA). The results of any two groups marked without the same alphabetic letters indicate a significant difference ($P < 0.05$); single and double asterisks indicate highly significant differences at $P < 0.01$ and $P < 0.001$, respectively.

Results

Effects of an IF-EMF (40 kHz) with various intensities on oocyte maturation

Initially, COCs were incubated in five IF-EMF intensities, including one control group (i.e., no MF), to evaluate the effects of IF-EMF on the IVM of porcine oocytes. Among the four EMF-treated groups, no significant differences ($P > 0.05$) in maturation rates were observed compared to the control group (74.20 ± 2.11%, 74.26 ± 2.12%, 80.50 ± 2.38%, and 78.21 ± 2.08% *vs.* 77.62 ± 2.02%, respectively) (Fig. 2).

Mitochondrial distribution in oocytes matured after exposure to IF-EMF

Nuclear maturation and cytoplasmic maturation are the two major criteria for measuring oocyte maturation. Mitochondrial distribution is one of the indicators of cytoplasmic maturation; therefore, mature

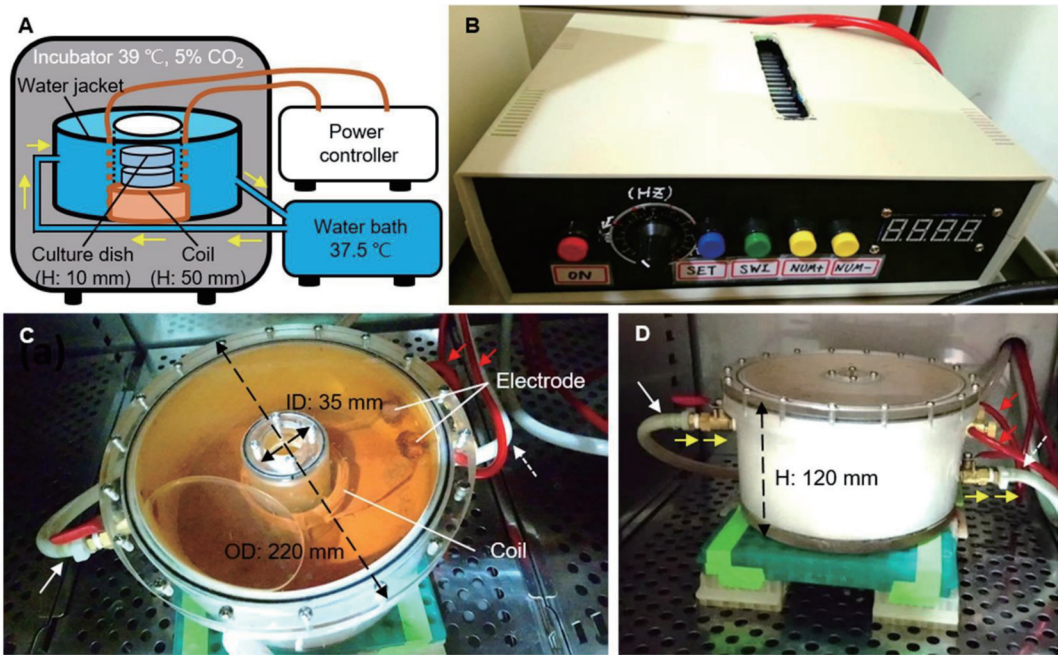

Fig. 1. The image of the EMF device. (A) The diagram depicts the EMF device setting in the incubator and connecting to the water bath outside the incubator. The coil (brown) set in a handmade water jacket is connected to the power controller. When power is on, the coil generates a magnetic field and excessive heat at the same time. The water (blue; yellow arrows indicate the direction of flow) with constant temperature (37.5ºC) from the water bath is driven by a water pump into the water jacket and then from the output returning to the water bath in order to maintain a constant culture environment (39ºC). (B) The power controller of the EMF device. The frequency of the IF-EMF is set to 40 kHz using a power controller. (C, D) Top and lateral views of the electromagnetic coil and its water jacket. The water jacket is set above the floor of the incubator on stainless racks to maintain a constant culture environment. The copper wires are covered with the red plastic tubes (red arrows) in connection with the power controller and twined to form a coil in the bottom of the acrylic box. In addition, two white plastic tubes for circulating warm water (input, white solid arrow) and heated water (output, white dotted arrow) are connected to the water jacket and the water bath, respectively. H: height, ID: inner diameter, OD: outer diameter.

Table 1. The intensities of the magnetic field at different positions within the magnetic field device

Distance from the bottom of device, cm	First measurement, G [1]	Second measurement, G [1]	Average of first and second measurements, G [2]
7	20.43 ± 3.79	17.63 ± 3.03	19.03 ± 3.63
6	38.81 ± 1.82	26.41 ± 1.57	32.61 ± 6.57
5	60.76 ± 2.04	48.40 ± 2.92	54.58 ± 6.80
4	88.59 ± 4.12	78.33 ± 2.83	83.46 ± 6.29
3	101.87 ± 3.75	100.54 ± 5.00	101.21 ± 4.36
2	115.95 ± 5.83	99.49 ± 4.69	107.72 ± 9.89
1	89.24 ± 6.58	90.71 ± 3.98	89.98 ± 5.34
0	69.92 ± 8.59	70.62 ± 3.81	70.27 ± 6.48

[1] Average of ten-time measurements at each position. [2] Average of twenty-time measurements at each position.

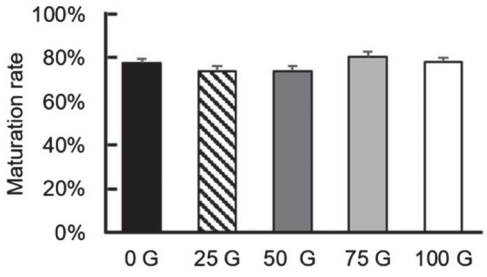

Fig. 2. Maturation rates of porcine oocytes under various IF-EMF exposures during IVM. The four IF-EMF treatment groups have no significant differences (P > 0.05) in maturation rates compared to the control group.

oocytes were stained with MitoTracker to observe mitochondrial patterns in the present study. Based on Gonzalez *et al*., peripheral, polarized, and diffused types of mitochondrial distribution patterns were adopted to classify mitochondrial patterns in the current study (Fig. 3A–F). The proportions of the three distribution patterns in each group are summarized in Fig. 3G. The oocytes in the 25 G group had a significantly lower proportion of mature mitochondrial patterns than the control and the 100 G groups (71.96 ± 3.22% *vs.* 93.61 ± 3.61% and 93.33 ± 6.67%, respectively), but not the 50 G and 75 G groups (83.33 ±12.02% and 82.50 ± 11.81%, respectively; Fig. 3H).

Distribution of cytoskeleton in matured oocytes after exposure to IF-EMF

The cytoskeleton distribution in IF-EMF-treated oocytes was observed after IVM. As shown in Fig. 4, it was observed in all five groups that spindle microtubules existed close to ooplamic chromosomes and the first polar body of matured oocytes, as well as microfilaments intensively localized around the position of the first polar body. No observable differences in cytoskeletal distribution patterns were found among the five groups treated with various IF-EMF intensities. Pro-metaphase II (PMII) and metaphase II (MII) oocytes showing distinct chromosomal alignments and microtubular

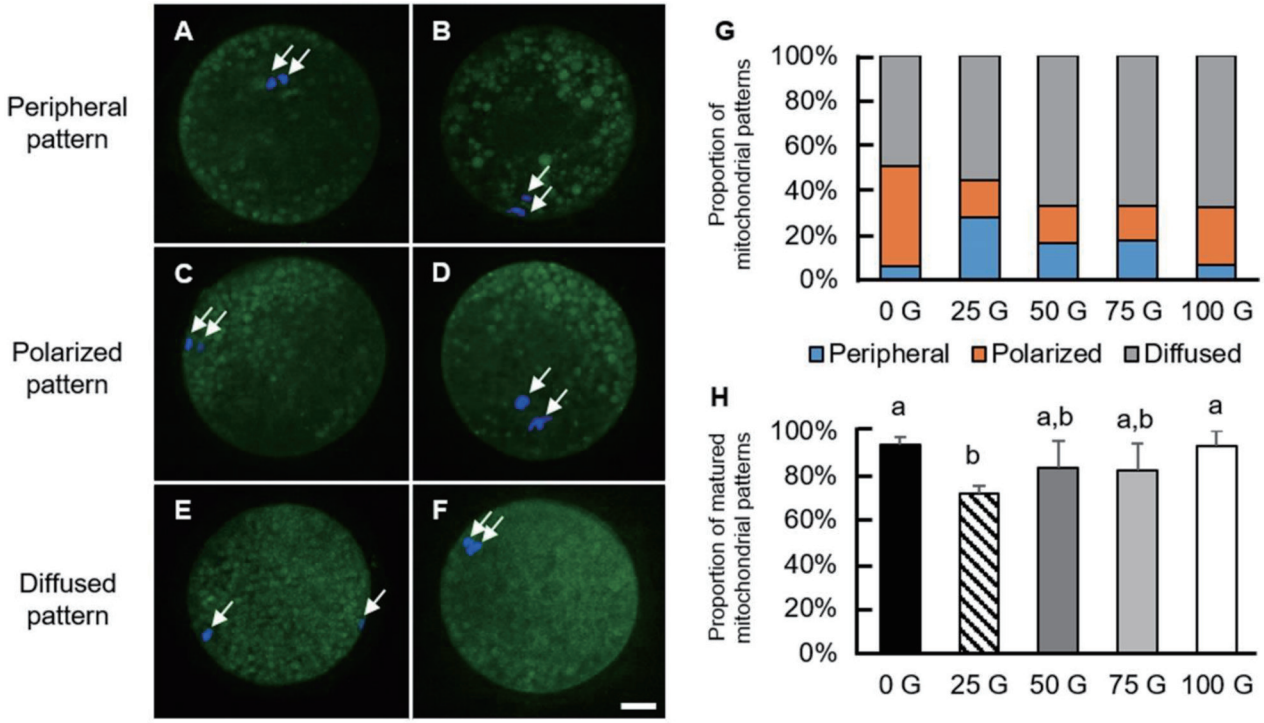

Fig. 3. The patterns and proportions of mitochondrial distribution in mature porcine oocytes. (A–F) Mature oocytes showing various patterns of mitochondrial distribution. Green: mitochondria, blue: chromosomes (white arrows). (A) and (B) are defined as peripheral patterns where mitochondria mainly are localized in the cortex of the oocytes. (C) and (D) are defined as polarized patterns, in which mitochondria aggregate at one side of the oocytes. Two types of polarized patterns were observed, with one localized near the chromosomes and the other being away from the chromosomes. (E) and (F) are defined as diffused patterns, in which mitochondria spread over the oocytes. (G) Oocytes exposed to various IF-EMF strengths show different patterns of mitochondrial distribution. (H) The proportion of most frequently observed patterns, i.e., polarized and diffused types, of mitochondrial distribution in mature oocytes of each treatment group are shown. The control and the 100 G-group have significantly higher percentages of frequently observed mitochondrial patterns than the 25 G-group. Scale bar: 25 μm.

patterns could be identified 44 h after the onset of IVM (Supplementary Fig. 1A–B). The chromosomes of some oocytes aligned on the metaphase plate with an aberrant morphology of spindle structure (Supplementary Fig. 1C–F); however, the proportions of abnormal microtubular patterns between the five groups were not significantly different ($P > 0.05$, Supplementary Table 1).

Expression of LC3B and mTOR in matured oocytes after IF-EMF exposure

It is also interesting to examine the autophagy of mature porcine oocytes after IF-EMF exposure. The most common autophagy markers are microtubule-associated protein 1 light chain 3β (MAP1LC3B or LC3B) and mammalian target of rapamycin (mTOR). The matured oocytes were fixed for immunofluorescence staining for autophagy markers, and the expression levels were quantified as the mean intensity (the fluorescence intensity in unit area) (Fig. 5). Both the 25 G- and the 50 G-treated groups had increased mean fluorescence intensities of LC3B compared to that of the control group (22.74 ± 2.12 and 17.45 ± 1.89 *vs.* 13.07 ± 0.88), instead of the 75 G- and the 100 G-treated groups (14.61 ± 1.26 and 15.07 ± 1.21, respectively). On the other hand, no significant differences in mTOR fluorescence expression were observed between all the IF-EMF-treated groups and the control group (37.76 ± 1.83, 37.20 ± 2.77, 34.33 ± 1.63, 33.63 ± 1.43 *vs.* 34.44 ± 1.43, $P > 0.05$).

Effects of exposure to various IF-EMF on early embryonic development

After oocyte maturation, the matured oocytes were electrically activated along with the kinase inhibitor 6-DMAP to evaluate the impact of IF-EMF on cleavage and blastocyst rates. Except for the 75 G- and 100 G-treatment groups (69.80 ± 3.27% and 68.31 ± 4.28%, respectively), the 25 G- and the 50 G-treated oocytes showed significantly lower ($P < 0.05$) cleavage rates than that of the control group (63.86 ± 4.57%, 63.23 ± 4.83% *vs.* 77.50 ± 3.48%, respectively; Fig. 6A). Similar to the cleavage rates, the 25 G- and the 50 G-treated groups also had decreased blastocyst rates compared to the control group (5.56 ± 1.22%, 7.27 ± 1.18% *vs.* 14.52 ± 2.96%, respectively), but not the 75 G- and the 100 G-treated groups (8.81 ± 2.14% and 9.32 ± 2.53%, respectively, $P > 0.05$; Fig. 6B). Unlike the cleavage rates and blastocyst rates, the total cell numbers of day 7 blastocysts (52.08 ± 3.20, 51.80 ± 6.97, 47.22 ± 6.59, 41.00 ± 6.10, and 38.21 ± 3.75 for the 0 G, 25 G, 50 G, 75 G, and 100 G-treated groups, respectively) had no differences among all treatment groups ($P > 0.05$, Fig. 7).

Discussion

The present study investigated the effects of exposure with 40 kHz IF-EMF at various intensities on porcine oocyte maturation and subsequent embryonic development after parthenogenetic activation. Compared to untreated control oocytes, lower IF-EMF intensities compromised blastocyst development rather than oocyte maturation.

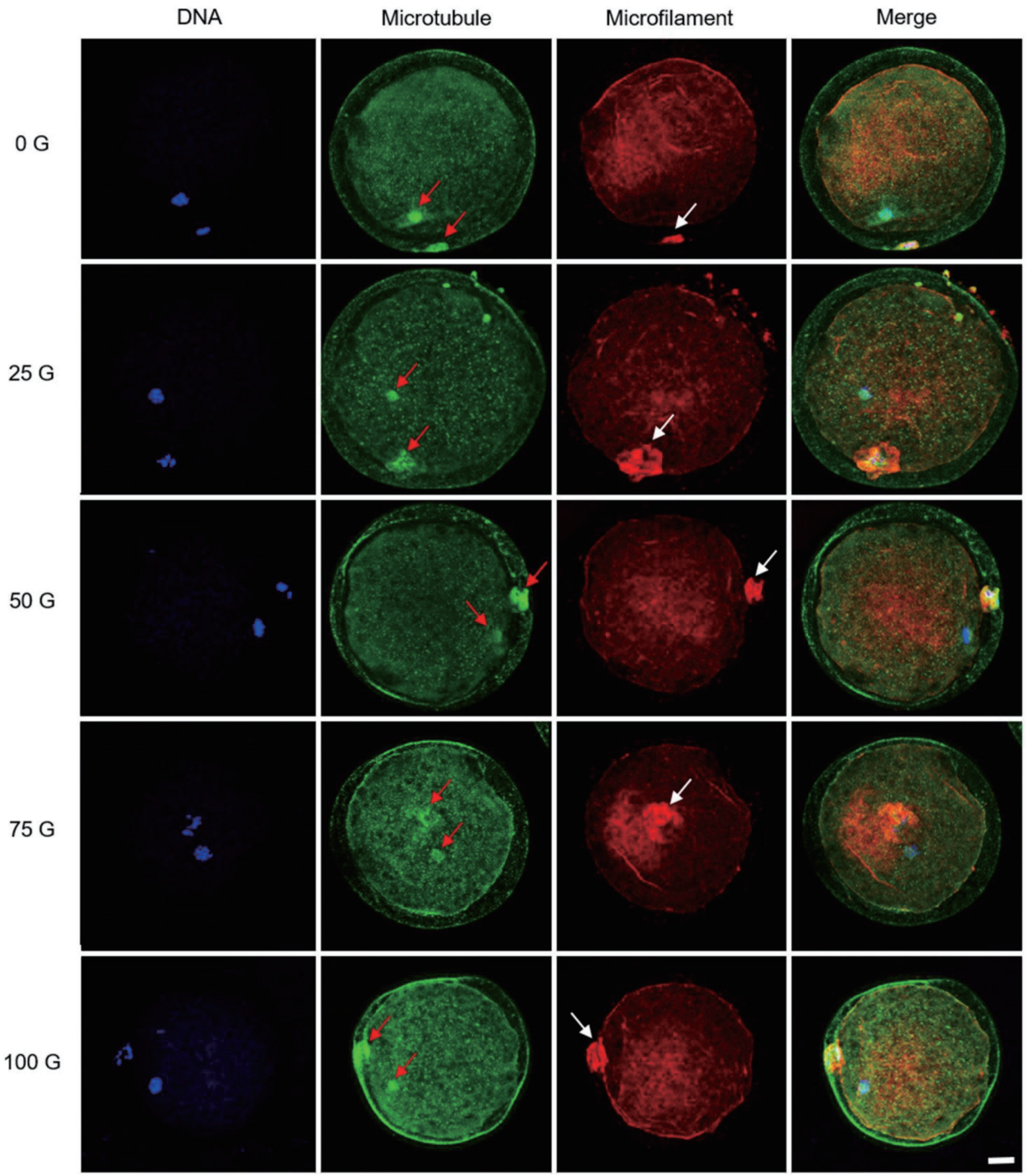

Fig. 4. Confocal microscopy of cytoskeleton distribution in mature porcine oocytes. The microtubules were distributed in the meiotic spindle of the oocytes and the first polar body (red arrows). The expression of microfilaments strongly localizes around the position of the first polar body (white arrows). No distinct alterations of these oocytes can be detected after treatment with various IF-EMFs. Blue: chromosomes; green: microtubules; red: microfilaments. Scale bar: 25 μm.

Even though the detrimental effects of IF-EMF did not immediately impact oocyte maturation, this effect appeared to be carried over to subsequent embryogenesis. Interestingly, exposure to IF-EMF also interfered with mitochondrial distribution and autophagy, which affected cytoplasmic maturation and deteriorated oocyte quality, which might partially explain the reduced cleavage and blastocyst rates of the low IF-EMF-treated groups. However, no discernible differences in cytoskeletal distribution and blastocyst cell number were observed among all groups, suggesting that most of the affected oocytes were incapable of forming blastocysts after parthenogenetic activation.

In the present study, no effects of various IF-EMF exposures on oocyte maturation were detected, but a negative effect emerged during the blastocyst formation stage. It is worth mentioning that the 25 G and 50 G groups had significantly reduced cleavage and blastocyst rates compared to the control group. Lower IF-EMF intensities interfere with early embryonic development more significantly, which

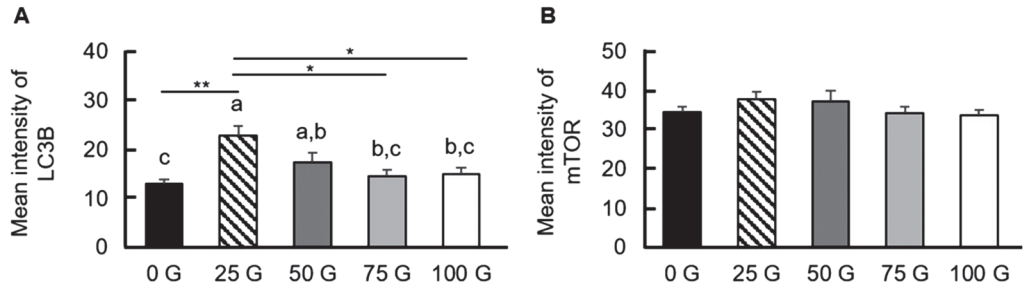

Fig. 5. Expression of autophagy markers LC3B and mTOR expressions in matured porcine oocytes. (A) The mean intensity of LC3B in oocytes exposed to various IF-EMF strengths. The 25 G- and the 50 G-groups show significantly higher LC3B intensities than the control group. (B) The mean intensity of mTOR in oocytes with various IF-EMF exposures. No significant difference can be detected in mTOR intensity among all treatment groups ($P > 0.05$).

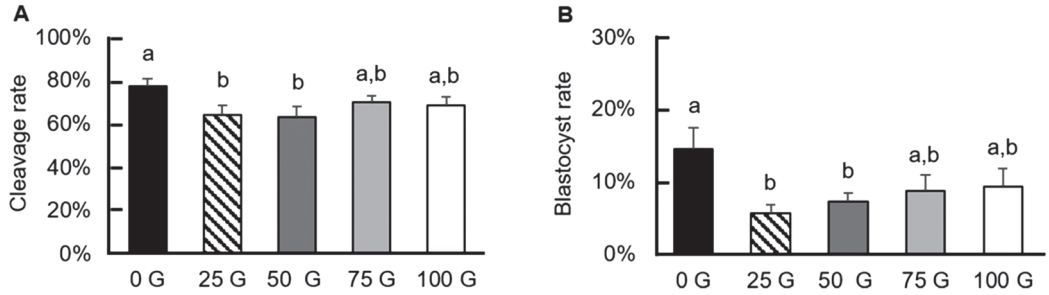

Fig. 6. Early embryonic development of various IF-EMF exposures on porcine oocytes during IVM followed by parthenogenetic activation. (A) Reduced cleavage rates (day 2) of the parthenotes are observed in the 25 G- and 50 G-treated groups compared to the control group. (B) The blastocyst formation rates at day 7 are also lower in the 25 G- and the 50 G-treatment groups than that of the control group.

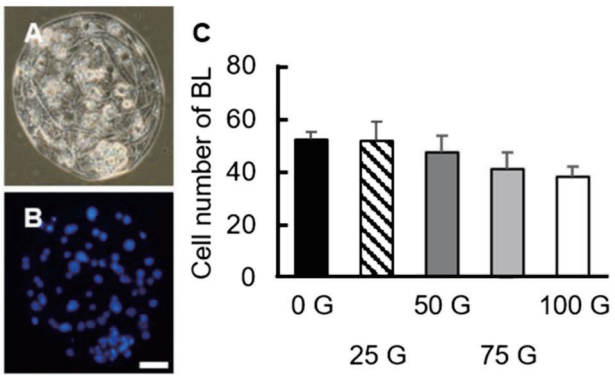

Fig. 7. Total cell numbers of day 7 porcine blastocysts in the various IF-EMF treatment groups. (A, B) The representative micrographs of the blastocyst embryos in bright field (A) and DAPI staining (B). Blue: nuclei. Scale bar: 25 µm. (C) Average total cell numbers of the blastocysts (day 7) in each treatment group after parthenogenetic activation. No difference between any two groups can be detected ($P > 0.05$). BL: blastocyst.

is inagreement with our expectation, i.e., a higher IF-EMF intensity would result in lower maturation, cleavage, or even blastocyst rates. As described above, none of the IF-EMF-treated groups differed in maturation rate from the control group. It is possible that the nuclear maturation of oocytes may not simply represent the effects of IF-EMF on oocyte maturation. Its subtle influence on cytoplasmic maturation or organelle localization could be adversely amplified during embryogenesis after parthenogenetic activation, perhaps even with sperm involvement. For the total cell number of the blastocysts (day 7), no differences were observed between any one of the four treatment groups and the control group. Although the control group had a higher blastocyst rate than other IF-EMF groups (i.e., the 25 G and the 50 G groups), the differences between blastomere proliferation rates were still undiscernible, possibly because of the well-known poor quality of pig embryos produced *in vitro*.

However, the reason the 25 G- and the 50 G-groups had the lowest cleavage and blastocyst rates under our experimental conditions is still unclear. Nevertheless, it is believed that lower-frequency EMFs are more bioactive than higher-frequency ones; in other words, low-frequency EMFs could exert more detrimental effects on cells or organisms. One study provided evidence to confirm this claim [27]. In addition, other studies have also suggested that the level of penetration in biological tissues is higher at the lower-frequency EMF [28, 29]. There was still a discrepancy between our results and those of previous studies because the EMF frequencies were the same (40 kHz) in all treatment groups in the present study.

A previous study suggested that the orientation or direction of the static EMF could affect tumor cell viability, but no discernible effects have been reported in other non-cancer cell types [30]. In the present study, it is also likely that oocytes cultured in different positions of the culture dish had different impacts from different orientations of the EMF relative to oocyte positions. In addition to the positional effect of the culture dishes in the IF-EMF device and the influence of AC from the power controller, it is also possible that the direction of MF is altered by the EMF-permeable metal incubator [5]. In other words, different directions of MFs could have

diverse effects on oocyte maturation or embryonic development. However, whether the MF direction potentially alters oogenesis or embryogenesis is difficult to verify in this study. Future work may focus on culturing oocytes at the same position with various EMF intensities and frequencies set from the power controller.

Complete oocyte maturation, including nuclear and cytoplasmic maturation, is critical for blastocyst formation. In addition to the nuclear maturation of oocytes, cytoplasmic maturation may refer to the redistribution of organelles, such as mitochondria, ribosomes, Golgi complex, endoplasmic reticulum, and cortical granules, and dynamic changes of the cytoskeleton, including microfilament and microtubule polymerization and depolymerization, which are associated with organelle migration, as well as the molecular maturation and metabolism of maturation-related mRNAs, proteins, and transcriptional factors [31].

As mentioned above, mitochondrial distribution is an essential indicator of cytoplasmic maturation. Variations in mitochondrial distribution during oocyte maturation have been reported in previous studies, which were associated with ATP production, regulation of calcium concentration, and redox homeostasis [32, 33]. The aggregation of mitochondria in the cortical region is the main feature of germinal vesicle (GV) stage oocytes. During porcine oocyte maturation, mitochondria dynamically migrate to the inner ooplasm and around the GV nucleus. A mature (MII) oocyte has a centrally localized distribution of mitochondria, with relatively fewer and larger mitochondrial foci and strong mitochondrial staining around the first polar body [32]. Many studies have indicated that EMF may disrupt redox homeostasis and the electron transport chain, thus causing mitochondrial dysfunction and ROS overexpression in reproductive cells or organisms [34–38]. In the present study, the number of mitochondria showing the most common type patterns, diffused and polarized types, of matured oocytes in the 25 G group was significantly less than in the control group. This finding strongly indicates that IF-EMF affects the distribution of mitochondria and, in turn, might interfere with the energy metabolism of mature porcine oocytes. Eventually, such an effect could indirectly retard blastocyst formation during early embryogenesis.

In addition to immunocytochemistry or epifluorescence microscopy, ultrastructures of mitochondria observed via transmission electron microscopy (TEM) can be used to evaluate oocyte quality [39]. It has been known that many conditions can cause morphological alterations or changes in the oocyte mitochondria. The mitochondrial morphology of oocytes alters during maturation and is species-specific. In pig oocytes, spherical mitochondria with few cristae are the main pattern of mitochondria observed before maturation, which presumably has only a low metabolic activity of energy [39]. Hooded mitochondria were rarely seen, in contrast to the more frequently existing shell-like and compartmentalized mitochondria in post-pubertal porcine oocytes [40, 41]. A previous study reported that EMF might induce morphological changes in mitochondrial cristae in human pancreatic cancer cells [42]. Changes in mitochondrial morphology of oocytes in several animal species have been associated with maternal age, as well as the activity of the electron transport chain for energy metabolism [39].

Mitochondrial dynamics, including fission, fusion, motility, crista shaping, and interactions with other organelles, enable cells or oocytes to adapt to stressful conditions, such as an over- or under-supply of nutrients, changes in intracellular calcium levels, and ROS [43]. Quantifying the RNA expression levels related to mitochondrial dynamics could also be used to evaluate mitochondrial activity.

In the present study, low IF-EMF intensities caused changes in the mitochondrial distribution patterns of porcine oocytes. It is conceivable that the cytoskeleton, including the microtubules and microfilaments, is the main contributor to the dragging of mitochondria to form various patterns. The cytoskeleton also participates in maturation processes, such as chromosome condensation, spindle formation and migration, polar body extrusion, and mitochondrial localization [44]. Therefore, we examined the changes in the cytoskeletal distribution of mature oocytes after exposure to various IF-EMF strengths. However, we did not detect any differences among the groups, similar to previous studies [44, 45]. A mature oocyte typically has most of its microtubules aggregated around the chromosomes to form the meiotic spindle. On the other hand, some microfilaments are anchored in the cortex of the ooplasm while some are particularly aggregated around the first polar body. Both the microtubules and the microfilaments of oocytes are distributed with little or only very few are observable in the cortical region of the ooplasm during the maturing or the MII stage [44, 45]. Based on previous studies, the cell cycle stages and microtubular patterns were used to evaluate the effect of the treatment on cytoskeletal distribution [46, 47]. In the present study, oocytes cultured for 44 h with the release of the first polar body, including PMII and MII oocytes, were defined as matured oocytes, but abnormal microtubule distributions in some MII oocytes could be observed. There were no significant differences in the cytoskeletal distribution observed in the proportions of PMII, MII, and even abnormal oocytes without the metaphase spindle in this experiment, suggesting no discernible influence on the cytoskeletal distribution of maturing oocytes exerted by IF-EMF under our experimental conditions.

Autophagy is a lysosome-dependent cell organelle recycling pathway involving the degradation of unnecessary or dysfunctional cell components to sustain cell viability with evolutionarily conservative mechanisms. It usually occurs in dying or starving cells and has been considered an active cell death pathway for decades [48–50]. The transport of cellular components by autophagosome trafficking during autophagy plays an important role in cell adaptation, anti-aging, and tumor repression [48]. Recent studies have proposed that autophagy activation reduces protein aggregation and organelle damage to maintain energy homeostasis and decreases ROS production to protect cells from apoptosis [51, 52]. Studies have shown that EMF exposure can activate autophagy [46, 53–56], mediated through ROS production and autophagy-related miRNA expression [50]. The expression of the surface marker of autophagosomes, LC3B, is positively correlated with autophagy activity [48], while mTOR is a negative regulator of autophagy [57]. Cellular autophagy can be triggered or activated when treated with mTOR inhibitors [58]. The 25 G and 50 G groups had higher LC3B expression than the control; besides, all treated groups showed no significant difference in mTOR expression compared to the control. Hence, our results suggest that the 25 G and 50 G groups had increased autophagy levels compared to the control group, depending on the integration of LC3B and mTOR expression. The results were somewhat out of our expectations. The four EMF treatment groups should have higher LC3B expression, but lower mTOR expression (i.e., autophagy activation) compared to the control group, with a dose-dependent effect. In effect, our findings showed decreased developmental potential in the 25 G- and the 50 G-treated oocytes compared to that of the control group, leading to only lower EMF intensities affecting oocyte cytoplasmic maturation mediated, possibly, by various degrees of autophagy.

Taken together, the impact of IF-EMF on female germ cells is poorly defined due to inconsistent or contradictory results from previous studies. Most likely, various IF-EMF intensities, frequen-

cies, duration of exposure, different animal model systems, and experimental protocols are among the potential factors that cause such inconsistencies [36]. Notably, the dose-effect relationship between IF-EMF exposure and porcine oocyte maturation and development was not strictly linear. Instead, exposure to lower intensity IF-EMF caused even more harmful effects on oocyte maturation by interrupting mitochondrial distribution and activating autophagy, affecting subsequent embryogenesis.

Conflict of interests: The authors have nothing to declare.

Acknowledgments

We wish to thank Siriya Phamoh, a Ph.D. student at the Department of Animal Science, National Chung Hsing University, Taiwan, for her help with ovary collection. Experiments and data analysis were performed in part using the Medical Research Core Facilities, Office of Research & Development at China Medical University (CMU), Taiwan. This work was partly supported by grants from the Ministry of Science and Technology, Taiwan (MOST109-2313-B-039-001), the CMU Hospital (DMR-108-128), and CMU (CMU109-MF-100).

References

1. **Bernabò N, Tettamanti E, Russo V, Martelli A, Turriani M, Mattoli M, Barboni B.** Extremely low frequency electromagnetic field exposure affects fertilization outcome in swine animal model. *Theriogenology* 2010; **73**: 1293–1305. [Medline] [CrossRef]
2. **Cecconi S, Gualtieri G, Di Bartolomeo A, Troiani G, Cifone MG, Canipari R.** Evaluation of the effects of extremely low frequency electromagnetic fields on mammalian follicle development. *Hum Reprod* 2000; **15**: 2319–2325. [Medline] [CrossRef]
3. **Kim J, Ha CS, Lee HJ, Song K.** Repetitive exposure to a 60-Hz time-varying magnetic field induces DNA double-strand breaks and apoptosis in human cells. *Biochem Biophys Res Commun* 2010; **400**: 739–744. [Medline] [CrossRef]
4. **Kim J, Yoon Y, Yun S, Park GS, Lee HJ, Song K.** Time-varying magnetic fields of 60 Hz at 7 mT induce DNA double-strand breaks and activate DNA damage checkpoints without apoptosis. *Bioelectromagnetics* 2012; **33**: 383–393. [Medline] [CrossRef]
5. **Song K, Im SH, Yoon YJ, Kim HM, Lee HJ, Park GS.** A 60 Hz uniform electromagnetic field promotes human cell proliferation by decreasing intracellular reactive oxygen species levels. *PLoS One* 2018; **13**: e0199753. [Medline] [CrossRef]
6. **Litvak E, Foster KR, Repacholi MH.** Health and safety implications of exposure to electromagnetic fields in the frequency range 300 Hz to 10 MHz. *Bioelectromagnetics* 2002; **23**: 68–82. [Medline] [CrossRef]
7. **Roivainen P, Eskelinen T, Jokela K, Juutilainen J.** Occupational exposure to intermediate frequency and extremely low frequency magnetic fields among personnel working near electronic article surveillance systems. *Bioelectromagnetics* 2014; **35**: 245–250. [Medline] [CrossRef]
8. **Yoshie S, Ogasawara Y, Ikehata M, Ishii K, Suzuki Y, Wada K, Wake K, Nakasono S, Taki M, Ohkubo C.** Evaluation of biological effects of intermediate frequency magnetic field on differentiation of embryonic stem cell. *Toxicol Rep* 2016; **3**: 135–140. [Medline] [CrossRef]
9. **Herrala M, Kumari K, Koivisto H, Luukkonen J, Tanila H, Naarala J, Juutilainen J.** Genotoxicity of intermediate frequency magnetic fields *in vitro* and *in vivo*. *Environ Res* 2018; **167**: 759–769. [Medline] [CrossRef]
10. **Shi D, Zhu C, Lu R, Mao S, Qi Y.** Intermediate frequency magnetic field generated by a wireless power transmission device does not cause genotoxicity *in vitro*. *Bioelectromagnetics* 2014; **35**: 512–518. [Medline] [CrossRef]
11. **Koyama S, Narita E, Shinohara N, Miyakoshi J.** Effect of an intermediate-frequency magnetic field of 23 kHz at 2 mT on chemotaxis and phagocytosis in neutrophil-like differentiated human HL-60 cells. *Int J Environ Res Public Health* 2014; **11**: 9649–9659. [Medline] [CrossRef]
12. **Sakurai T, Narita E, Shinohara N, Miyakoshi J.** Intermediate frequency magnetic field at 23 kHz does not modify gene expression in human fetus-derived astroglia cells. *Bioelectromagnetics* 2012; **33**: 662–669. [Medline] [CrossRef]
13. **Nishimura I, Oshima A, Shibuya K, Mitani T, Negishi T.** Acute and subchronic toxicity of 20 kHz and 60 kHz magnetic fields in rats. *J Appl Toxicol* 2016; **36**: 199–210. [Medline] [CrossRef]
14. **Kim SH, Lee HJ, Choi SY, Gimm YM, Pack JK, Choi HD, Lee YS.** Toxicity bioassay in Sprague-Dawley rats exposed to 20 kHz triangular magnetic field for 90 days. *Bioelectromagnetics* 2006; **27**: 105–111. [Medline] [CrossRef]
15. **Kumari K, Capstick M, Cassara AM, Herrala M, Koivisto H, Naarala J, Tanila H, Viluksela M, Juutilainen J.** Effects of intermediate frequency magnetic fields on male fertility indicators in mice. *Environ Res* 2017; **157**: 64–70. [Medline] [CrossRef]
16. **Nishimura I, Oshima A, Shibuya K, Mitani T, Negishi T.** Absence of reproductive and developmental toxicity in rats following exposure to a 20-kHz or 60-kHz magnetic field. *Regul Toxicol Pharmacol* 2012; **64**: 394–401. [Medline] [CrossRef]
17. **Nishimura I, Imai S, Negishi T.** Lack of chick embryotoxicity after 20 kHz, 1.1 mT magnetic field exposure. *Bioelectromagnetics* 2009; **30**: 573–582. [Medline] [CrossRef]
18. **Nishimura I, Tanaka K, Negishi T.** Intermediate frequency magnetic field and chick embryotoxicity. *Congenit Anom (Kyoto)* 2013; **53**: 115–121. [Medline] [CrossRef]
19. **Klug S, Hetscher M, Giles S, Kohlsmann S, Kramer K.** The lack of effects of nonthermal RF electromagnetic fields on the development of rat embryos grown in culture. *Life Sci* 1997; **61**: 1789–1802. [Medline] [CrossRef]
20. **Nishimura I, Oshima A, Shibuya K, Negishi T.** Lack of teratological effects in rats exposed to 20 or 60 kHz magnetic fields. *Birth Defects Res B Dev Reprod Toxicol* 2011; **92**: 469–477. [Medline] [CrossRef]
21. **Lee HJ, Pack JK, Gimm YM, Choi HD, Kim N, Kim SH, Lee YS.** Teratological evaluation of mouse fetuses exposed to a 20 kHz EMF. *Bioelectromagnetics* 2009; **30**: 330–333. [Medline] [CrossRef]
22. **Khan MW, Roivainen P, Herrala M, Tiikkaja M, Sallmén M, Hietanen M, Juutilainen J.** A pilot study on the reproductive risks of maternal exposure to magnetic fields from electronic article surveillance systems. *Int J Radiat Biol* 2018; **94**: 902–908. [Medline] [CrossRef]
23. **Gilchrist RB, Thompson JG.** Oocyte maturation: emerging concepts and technologies to improve developmental potential *in vitro*. *Theriogenology* 2007; **67**: 6–15. [Medline] [CrossRef]
24. **González R, Sjunnesson YCB.** Effect of blood plasma collected after adrenocorticotropic hormone administration during the preovulatory period in the sow on oocyte *in vitro* maturation. *Theriogenology* 2013; **80**: 673–683. [Medline] [CrossRef]
25. **Brevini TAL, Vassena R, Francisci C, Gandolfi F.** Role of adenosine triphosphate, active mitochondria, and microtubules in the acquisition of developmental competence of parthenogenetically activated pig oocytes. *Biol Reprod* 2005; **72**: 1218–1223. [Medline] [CrossRef]
26. **Pawlak P, Chabowska A, Malyszka N, Lechniak D.** Mitochondria and mitochondrial DNA in porcine oocytes and cumulus cells—A search for developmental competence marker. *Mitochondrion* 2016; **27**: 48–55. [Medline] [CrossRef]
27. **Panagopoulos DJ, Karabarbounis A, Margaritis LH.** Mechanism for action of electromagnetic fields on cells. *Biochem Biophys Res Commun* 2002; **298**: 95–102. [Medline] [CrossRef]
28. **Serway RA, Jewett JWJ.** Principles of physics: a calculus-based text (5th edition). Pacific Grove, CA, US: Brooks/Cole; 2013.
29. **World Health Organization.** Establishing a Dialogue on Risks from Electromagnetic Fields, World health Organization 2002, Geneva, Switzerland; 2002.
30. **Tian X, Wang D, Zha M, Yang X, Ji X, Zhang L, Zhang X.** Magnetic field direction differentially impacts the growth of different cell types. *Electromagn Biol Med* 2018; **37**: 114–125. [Medline] [CrossRef]
31. **Ferreira EM, Vireque AA, Adona PR, Meirelles FV, Ferriani RA, Navarro PAAS.** Cytoplasmic maturation of bovine oocytes: structural and biochemical modifications and acquisition of developmental competence. *Theriogenology* 2009; **71**: 836–848. [Medline] [CrossRef]
32. **Sun QY, Wu GM, Lai L, Park KW, Cabot R, Cheong HT, Day BN, Prather RS, Schatten H.** Translocation of active mitochondria during pig oocyte maturation, fertilization and early embryo development *in vitro*. *Reproduction* 2001; **122**: 155–163. [Medline] [CrossRef]
33. **Dumollard R, Duchen M, Carroll J.** The role of mitochondrial function in the oocyte and embryo. *Curr Top Dev Biol* 2007; **77**: 21–49. [Medline] [CrossRef]
34. **Santini SJ, Cordone V, Falone S, Mijit M, Tatone C, Amicarelli F, Di Emidio G.** Role of mitochondria in the oxidative stress induced by electromagnetic fields: focus on reproductive systems. *Oxid Med Cell Longev* 2018; **2018**: 5076271. [Medline] [CrossRef]
35. **Sangun O, Dundar B, Darici H, Comlekci S, Doguc DK, Celik S.** The effects of long-term exposure to a 2450 MHz electromagnetic field on growth and pubertal development in female Wistar rats. *Electromagn Biol Med* 2015; **34**: 63–71. [Medline] [CrossRef]
36. **Burlaka A, Tsybulin O, Sidorik E, Lukin S, Polishuk V, Tsehmistrenko S, Yakymenko I.** Overproduction of free radical species in embryonal cells exposed to low intensity radiofrequency radiation. *Exp Oncol* 2013; **35**: 219–225. [Medline]
37. **Pandey N, Giri S, Das S, Upadhaya P.** Radiofrequency radiation (900 MHz)-induced DNA damage and cell cycle arrest in testicular germ cells in swiss albino mice. *Toxicol Ind Health* 2017; **33**: 373–384. [Medline] [CrossRef]
38. **Hagras AM, Toraih EA, Fawzy MS.** Mobile phones electromagnetic radiation and NAD^+-dependent isocitrate dehydrogenase as a mitochondrial marker in asthenozoospermia. *Biochim Open* 2016; **3**: 19–25. [Medline] [CrossRef]
39. **Reader KL, Stanton JL, Juengel JL.** The role of oocyte organelles in determining developmental competence. *Biology (Basel)* 2017; **6**: 35. [Medline]
40. **Pedersen HS, Callesen H, Løvendahl P, Chen F, Nyengaard JR, Nikolaisen NK, Holm P, Hyttel P.** Ultrastructure and mitochondrial numbers in pre- and postpubertal pig oocytes. *Reprod Fertil Dev* 2016; **28**: 586–598. [Medline] [CrossRef]
41. **Kere M, Liu PC, Chen YK, Chao PC, Tsai LK, Yeh TY, Siriboon C, Intawicha P, Lo NW, Chiang HI, Fan YK, Ju JC.** Ultrastructure characterization of porcine growing and

in vitro matured oocytes. *Animals (Basel)* 2020; **10**: 664. [Medline] [CrossRef]

42. **Curley SA, Palalon F, Lu X, Koshkina NV.** Noninvasive radiofrequency treatment effect on mitochondria in pancreatic cancer cells. *Cancer* 2014; **120**: 3418–3425. [Medline] [CrossRef]
43. **Eisner V, Picard M, Hajnóczky G.** Mitochondrial dynamics in adaptive and maladaptive cellular stress responses. *Nat Cell Biol* 2018; **20**: 755–765. [Medline] [CrossRef]
44. **Sun QY, Lai L, Park KW, Kühholzer B, Prather RS, Schatten H.** Dynamic events are differently mediated by microfilaments, microtubules, and mitogen-activated protein kinase during porcine oocyte maturation and fertilization *in vitro*. *Biol Reprod* 2001; **64**: 879–889. [Medline] [CrossRef]
45. **Suzuki H, Saito Y.** Cumulus cells affect distribution and function of the cytoskeleton and organelles in porcine oocytes. *Reprod Med Biol* 2006; **5**: 183–194. [Medline] [CrossRef]
46. **Roeles J, Tsiavaliaris G.** Actin-microtubule interplay coordinates spindle assembly in human oocytes. *Nat Commun* 2019; **10**: 4651. [Medline] [CrossRef]
47. **Ding ZM, Hua LP, Ahmad MJ, Safdar M, Chen F, Wang YS, Zhang SX, Miao YL, Xiong JJ, Huo LJ.** Diethylstilbestrol exposure disrupts mouse oocyte meiotic maturation *in vitro* through affecting spindle assembly and chromosome alignment. *Chemosphere* 2020; **249**: 126182. [Medline] [CrossRef]
48. **Shen XH, Jin YX, Liang S, Kwon JW, Zhu JW, Lei L, Kim NH.** Autophagy is required for proper meiosis of porcine oocytes maturing *in vitro*. *Sci Rep* 2018; **8**: 12581. [Medline] [CrossRef]
49. **Lee SH, Hiradate Y, Hoshino Y, Tanemura K, Sato E.** Quantitative analysis in LC3-II protein *in vitro* maturation of porcine oocyte. *Zygote* 2014; **22**: 404–410. [Medline] [CrossRef]
50. **Hao YH, Zhao L, Peng RY.** Effects of electromagnetic radiation on autophagy and its regulation. *Biomed Environ Sci* 2018; **31**: 57–65. [Medline]
51. **Li L, Zhang Q, Tan J, Fang Y, An X, Chen B.** Autophagy and hippocampal neuronal injury. *Sleep Breath* 2014; **18**: 243–249. [Medline] [CrossRef]
52. **Gozuacik D, Akkoc Y, Ozturk DG, Kocak M.** Autophagy-Regulating microRNAs and Cancer. *Front Oncol* 2017; **7**: 65. [Medline] [CrossRef]
53. **Jiang DP, Li JH, Zhang J, Xu SL, Kuang F, Lang HY, Wang YF, An GZ, Li J, Guo GZ.** Long-term electromagnetic pulse exposure induces Abeta deposition and cognitive dysfunction through oxidative stress and overexpression of APP and BACE1. *Brain Res* 2016; **1642**: 10–19. [Medline] [CrossRef]
54. **Marchesi N, Osera C, Fassina L, Amadio M, Angeletti F, Morini M, Magenes G, Venturini L, Biggiogera M, Ricevuti G, Govoni S, Caorsi S, Pascale A, Comincini S.** Autophagy is modulated in human neuroblastoma cells through direct exposition to low frequency electromagnetic fields. *J Cell Physiol* 2014; **229**: 1776–1786. [Medline] [CrossRef]
55. **Liu K, Zhang G, Wang Z, Liu Y, Dong J, Dong X, Liu J, Cao J, Ao L, Zhang S.** The protective effect of autophagy on mouse spermatocyte derived cells exposure to 1800 MHz radiofrequency electromagnetic radiation. *Toxicol Lett* 2014; **228**: 216–224. [Medline] [CrossRef]
56. **Koshkina NV, Briggs K, Palalon F, Curley SA.** Autophagy and enhanced chemosensitivity in experimental pancreatic cancers induced by noninvasive radiofrequency field treatment. *Cancer* 2014; **120**: 480–491. [Medline] [CrossRef]
57. **Lee J, Park JI, Yun JI, Lee Y, Yong H, Lee ST, Park CK, Hyun SH, Lee GS, Lee E.** Rapamycin treatment during *in vitro* maturation of oocytes improves embryonic development after parthenogenesis and somatic cell nuclear transfer in pigs. *J Vet Sci* 2015; **16**: 373–380. [Medline] [CrossRef]
58. **Sully K, Akinduro O, Philpott MP, Naeem AS, Harwood CA, Reeve VE, O'Shaughnessy RF, Byrne C.** The mTOR inhibitor rapamycin opposes carcinogenic changes to epidermal Akt1/PKBα isoform signaling. *Oncogene* 2013; **32**: 3254–3262. [Medline] [CrossRef]